

A Temporal Difference Method for Stochastic Continuous Dynamics

Haruki Settai

University of Tokyo

settai-haruki692@g.ecc.u-tokyo.ac.jp

Naoya Takeishi

University of Tokyo

ntake@g.ecc.u-tokyo.ac.jp

Takehisa Yairi

University of Tokyo

yairi@g.ecc.u-tokyo.ac.jp

Abstract

For continuous systems modeled by dynamical equations such as ODEs and SDEs, Bellman’s principle of optimality takes the form of the Hamilton-Jacobi-Bellman (HJB) equation, which provides the theoretical target of reinforcement learning (RL). Although recent advances in RL successfully leverage this formulation, the existing methods typically assume the underlying dynamics are known a priori because they need explicit access to the coefficient functions of dynamical equations to update the value function following the HJB equation. We address this inherent limitation of HJB-based RL; we propose a model-free approach still targeting the HJB equation and propose the corresponding temporal difference method. We demonstrate its potential advantages over transition kernel-based formulations, both qualitatively and empirically. The proposed formulation paves the way toward bridging stochastic optimal control and model-free reinforcement learning.

1 Introduction

Reinforcement learning (RL) has been successfully applied in various domains, ranging from discrete systems like board games (Silver et al., 2018) to systems that are continuous in both state and time such as robotic control (Kober et al., 2013). RL research has been advancing through a variety of approaches, and much of the work has focused on improving methods by refining objective functions (Schulman et al., 2015, 2017), balancing exploration and exploitation (Haarnoja et al., 2018), and developing more effective architectures (Hafner et al., 2019). These efforts have significantly advanced the field, leading to the development of various successful algorithms.

In contrast to the studies primarily targeting algorithmic components or optimization techniques, we focus on the continuity of time and explore what we call continuous RL, where the dynamics of systems are described by ordinary differential equations (ODEs) or stochastic differential equations (SDEs), which is a relatively underexplored aspect of RL. Although many RL methods have been applied, sometimes heuristically, to both discrete and continuous systems, the continuity of the system has not necessarily been fully exploited, even when it is known in advance. Laying a foundation for utilizing prior knowledge of continuity is important toward more effective learning and decision-making methods, particularly for practical applications such as robot control and autonomous driving, which typically fall into the target of continuous RL.

A way to incorporate prior knowledge of the system’s continuity into the learning process is to use the Hamilton-Jacobi-Bellman (HJB) equation. In the Bellman equation, continuity is encoded in the transition

kernel. However, in model-free RL, where transitions are approximated using samples, this continuity information is lost because the transition kernel is not explicitly modeled. On the other hand, the HJB equation retains the continuity information in the argument of the expectation rather than in the transition kernel. This property allows the HJB equation to keep taking continuity into account even under sample-based approximations. However, because the HJB equation depends on the coefficient functions of the system’s dynamics, prior work has largely been limited to model-based approaches (Munos and Bourgine, 1997; Yildiz et al., 2021).

In this paper, we introduce a temporal difference (TD) method based on the HJB equation, namely *differential TD* (dTD), achieved through sample-based approximation of the expectation term in the HJB equation. dTD enables policy evaluation without requiring knowledge or estimation of the system dynamics, while incorporating the continuity of the dynamics into the learning process. It is compatible with on-policy methods such as A2C (Mnih et al., 2016) and PPO (Schulman et al., 2017), and we demonstrate its effectiveness on Mujoco (Todorov et al., 2012) tasks including Hopper, HalfCheetah, Ant, and Humanoid. The codes for the proposed method are available at https://github.com/4thhia/differential_TD.

2 Related Work

Deterministic Dynamics The study of continuous RL for ODE systems can be traced back to studies such as Baird (1994); Munos (1997); Doya (2000); Munos (2006). Baird (1994) discovered that the Q-function collapses in continuous RL, which was rigorously proven and extended to deep RL in Tallec et al. (2019). In Munos (1997), model-free approaches for ODE systems were first studied. Doya (2000) was the first to introduce TD for ODE systems and extended it to $TD(\lambda)$ and actor-critic. Munos (2006) investigated the estimation of policy gradients for ODE systems and proposed a pathwise derivative approach. More recently, Vamvoudakis and Crofton (2017) developed a model-free RL framework for deterministic linear systems. Kim et al. (2021) proposed a model-free Q-learning approach in which the control is derived from the HJB equation, while the learning target is based on the conventional Bellman equation. Yildiz et al. (2021) introduced a model-based method that leverages the Neural ODE framework to enable continuous-time optimization using learned system dynamics.

Stochastic Dynamics One of the earliest works on RL in SDE systems is Munos and Bourgine (1997), which takes a model-based approach. However, research in this direction remained largely unexplored until recently. In the past few years, a growing body of work has emerged that aims to establish theoretical foundations for RL in stochastic dynamics. Wang et al. (2020) introduced an entropy-regularized relaxed control formulation and provided a comprehensive analysis in the LQR setting. Tang et al. (2022) further demonstrated the well-posedness of the HJB equation within this relaxed control framework. Jia and Zhou (2022a) showed that Bellman optimality is equivalent to maintaining the martingale property of a suitably defined stochastic process, and proposed a corresponding algorithm. However, their method requires access to full trajectory information and thus applies only to finite-horizon settings. Building on this approach, Jia and Zhou (2022b, 2023) proposed actor-critic and Q-learning algorithms for finite-horizon SDE systems, respectively. Zhao et al. (2023) extended key theoretical tools such as the state visitation distribution and the performance difference lemma to the continuous-time setting and applied them to TRPO and PPO. Independently, Kobeissi and Bach (2023) proposed a variance-reduction technique for policy evaluation.

While HJB-based formulations have been extensively studied, existing model-free approaches inevitably resort to transition kernel representations, which obscure the information that the dynamics are continuous. We instead propose a model-free method grounded in stochastic dynamics that remains computationally tractable across broader tasks.

3 Background

3.1 Problem Setting

We consider a continuous RL setting where the state space is $\mathcal{S} \subset \mathbb{R}^n$ and the action space is \mathcal{A} . We suppose that the dynamics of the state are governed by the following controlled SDE:

$$dS_t = \mu(S_t, A_t)dt + \sigma(S_t, A_t)dB_t, \quad (1)$$

where $\mu : \mathcal{S} \times \mathcal{A} \rightarrow \mathbb{R}^n$, $\sigma : \mathcal{S} \times \mathcal{A} \rightarrow \mathbb{R}^{n \times m}$, and $(B_t)_{t \geq 0}$ is the m -dimensional Brownian motion. Note that the state evolution is influenced by both the inherent noise in the system as well as the randomness induced by the stochastic policy $\pi : \mathcal{S} \rightarrow \mathcal{P}(\mathcal{A})$, where $\mathcal{P}(\mathcal{A})$ is the space of probability distribution over the action space. Thus, the expectation related to this SDE is expressed as $\mathbb{E}_{p_\pi}[\cdot]$, where p_π denotes the transition probability density function corresponding to this SDE. For simplicity, we assume that the stochastic process (1) is well-defined; see Appendix A.1 for a detailed justification. We here focus on SDE systems because we can recover results for ODE systems in the limit of $\sigma = 0$.

3.2 Continuous RL

The goal of continuous RL is to find the policy π^* that maximizes the infinite horizon expected discounted cumulative reward:

$$\pi^*(s) = \operatorname{argmax}_{\pi} \mathbb{E}_{p_\pi} \left[\int_0^\infty e^{-\gamma t} \rho(S_t, A_t) dt \mid S_0 = s \right],$$

where $\rho : \mathcal{S} \times \mathcal{A} \rightarrow \mathbb{R}$ is the reward rate function, and $\gamma \in (0, \infty)$ is a constant discount factor. Throughout the paper we assume that ρ is continuous in its respective arguments and bounded, an assumption used in establishing the well-posedness of the associated HJB equation (see Appendix A.1).

A typical approach for finding π^* is to use the optimal value function, which is defined as follows:

$$V^*(s) := \max_{\pi} \mathbb{E}_{p_\pi} \left[\int_t^\infty e^{-\gamma(\tau-t)} \rho(S_\tau, A_\tau) d\tau \mid S_t = s \right].$$

In a continuous-time MDP, π^* can be found by solving the Bellman equation:

$$V^*(s_t) = \max_{\pi} \mathbb{E}_{p_\pi} [\rho(s_t, A_t) \Delta t + e^{-\gamma \Delta t} V^*(S_{t+\Delta t})], \quad (2)$$

where Δt is a small time interval and need not be constant. Similarly to standard discrete RL, this problem can be solved in a model-free setting by approximating the expectation on the right-hand side with samples and performing value iteration. However, in (2), the fact that the system follows an SDE is encoded only in the transition probability density (i.e., the subscript of the expectation), so dropping it by sample-based approximation disregards the prior knowledge of continuity and thus does not necessarily leverage the information.

3.3 HJB equation

Since an agent depends only on observations and update rules, a natural way to inform the agent that the system follows an SDE is to incorporate the SDE into the update rules. This can be achieved by further transforming (2) using the SDE (i.e., expanding $V(S_{t+\Delta t})$ via the Ito formula), resulting in the well-known

HJB equation (see Appendix A.2 for more detail):

$$V^*(s_t) = \frac{1}{\gamma} \max_{\pi} \mathbb{E}_{p_{\pi}} \left[\rho(s_t, A_t) + \sum_{i=1}^n \mu^i(s_t, A_t) \frac{\partial V^*(s)}{\partial s^i} \Big|_{s=s_t} + \frac{1}{2} \sum_{i=1}^n \sum_{j=1}^n [\sigma(s_t, A_t) \sigma^{\top}(s_t, A_t)]^{ij} \frac{\partial^2 V^*(s)}{\partial s^i \partial s^j} \Big|_{s=s_t} \right], \quad (3)$$

where μ^i and $[\sigma \sigma^{\top}]^{ij}$ denote the i -th element of μ and the (i, j) -th element of $\sigma \sigma^{\top}$, respectively.

4 Deriving TD for Continuous Systems

Now, are we all ready to implement model-free value iteration just by approximating the expectation on the right-hand side of (3) with samples? The answer is no because the argument of the expectation includes the coefficient functions of the SDE, μ and σ , making it impossible to directly approximate the expectation with samples. In this section, we first propose a way to derive a TD from the HJB equation and then verify a key theoretical property—namely, the contractivity of the resulting operator—which underpins the applicability of standard TD learning theories.

4.1 Deriving TD from the HJB equation

To utilize HJB for model-free RL, we need to transform the argument of the expectation on the right-hand side of equation (3) into a sample-based expression. For this purpose, while many previous studies employed value iteration-based methods using the optimal value function, we adopt a policy iteration-based approach based on the value function for a fixed policy:

$$V^{\pi}(s) := \mathbb{E}_{p_{\pi}} \left[\int_t^{\infty} e^{-\gamma(\tau-t)} \rho(S_{\tau}, A_{\tau}) d\tau \mid S_t = s \right].$$

Later we will discuss this choice more. The HJB equation under a fixed policy is

$$V^{\pi}(s_t) = \frac{1}{\gamma} \mathbb{E}_{p_{\pi}} \left[\rho(s_t, A_t) + \sum_{i=1}^n \mu^i(s_t, A_t) \frac{\partial V^{\pi}(s)}{\partial s^i} \Big|_{s_t} + \frac{1}{2} \sum_{i=1}^n \sum_{j=1}^n [\sigma(s_t, A_t) \sigma^{\top}(s_t, A_t)]^{ij} \frac{\partial^2 V^{\pi}(s)}{\partial s^i \partial s^j} \Big|_{s_t} \right]. \quad (4)$$

We now present our main theoretical result. It gives the foundation for our model-free formulation of temporal-difference learning based on the HJB equation. The idea is that the drift and diffusion terms in the HJB equation can be equivalently expressed using limits of sample-based finite differences.

Proposition 1. *When a stochastic process $(S_t)_{t \geq 0}$ follows the SDE in (1), we have*

$$\mathbb{E}_{p_{\pi}} [\mu^i(s_t, A_t)] = \lim_{\Delta t \rightarrow 0} \mathbb{E}_{p_{\pi}} \left[\frac{S_{t+\Delta t}^i - s_t^i}{\Delta t} \right] \quad (5)$$

and

$$\mathbb{E}_{p_{\pi}} [\sigma(s_t, A_t) \sigma^{\top}(s_t, A_t)]^{ij} = \lim_{\Delta t \rightarrow 0} \mathbb{E}_{p_{\pi}} \left[\frac{(S_{t+\Delta t}^i - s_t^i)(S_{t+\Delta t}^j - s_t^j)}{\Delta t} \right]. \quad (6)$$

Proof. For the first claim, we expand the i -th component of the SDE (1) using the Ito formula:

$$S_{t+\Delta t}^i = s_t^i + \mu^i(s_t, A_t)\Delta t + \sum_{j=1}^m \sigma^{ij}(s_t, A_t)(B_{t+\Delta t}^j - B_t^j) + O(\Delta t^{\frac{3}{2}}). \quad (7)$$

Since $B_{t+\Delta t}^j - B_t^j$ follows a zero-mean Gaussian and is independent of the state and the action,

$$\mathbb{E}_{p_\pi} \left[\sum_{j=1}^m \sigma^{ij}(s_t, A_t)(B_{t+\Delta t}^j - B_t^j) \right] = \sum_{j=1}^m \mathbb{E}_\pi [\sigma^{ij}(s_t, A_t)] \mathbb{E} [B_{t+\Delta t}^j - B_t^j] = 0.$$

By taking the expectation of both sides of (7) and then letting $\Delta t \rightarrow 0$, the terms in $O(\Delta t^{\frac{3}{2}})$ vanish, and we obtain (5). For the second part of the claim, we begin by considering the product:

$$\begin{aligned} & (S_{t+\Delta t}^i - s_t^i)(S_{t+\Delta t}^j - s_t^j) \\ &= \mu^i(s_t, A_t)\mu^j(s_t, A_t)\Delta t^2 + \sum_{k=1}^m \sum_{l=1}^m \sigma^{ik}(s_t, A_t)\sigma^{jl}(s_t, A_t)(B_{t+\Delta t}^k - B_t^k)(B_{t+\Delta t}^l - B_t^l) \\ & \quad + \mu^i(s_t, A_t)\Delta t \sum_{k=1}^m \sigma^{jk}(s_t, A_t)(B_{t+\Delta t}^k - B_t^k) + \mu^j(s_t, A_t)\Delta t \sum_{k=1}^m \sigma^{ik}(s_t, A_t)(B_{t+\Delta t}^k - B_t^k). \end{aligned} \quad (8)$$

and then take the expectation of both sides. Using the fact

$$\mathbb{E} [(B_{t+\Delta t}^k - B_t^k)(B_{t+\Delta t}^l - B_t^l)] = \delta_{kl}\Delta t,$$

where $\delta_{kl} = 1$ if $k = l$ and $\delta_{kl} = 0$ otherwise, we can take the expectation of both sides of equation (8) and then let $\Delta t \rightarrow 0$, which yields (6). \square

Remark 1. Note that since $S_{t+\Delta t}$ in equations (5) and (6) is sampled under the policy π , our method is not applicable to off-policy settings such as value iteration or Q -learning. This limitation reflects a fundamental distinction: our formulation relies on the HJB equation under a fixed policy (i.e., policy evaluation), rather than the classical HJB equation involving maximization over all policies.

From Proposition 1, the HJB equation (4) can be reformulated as

$$\begin{aligned} V^\pi(s_t) = & \frac{1}{\gamma} \lim_{\Delta t \rightarrow 0} \mathbb{E}_{p_\pi} \left[\rho(s_t, A_t) + \sum_{i=1}^n \frac{S_{t+\Delta t}^i - s_t^i}{\Delta t} \frac{\partial V^\pi(s)}{\partial s^i} \Big|_{s_t} \right. \\ & \left. + \frac{1}{2} \sum_{i=1}^n \sum_{j=1}^n \frac{(S_{t+\Delta t}^i - s_t^i)(S_{t+\Delta t}^j - s_t^j)}{\Delta t} \frac{\partial^2 V^\pi(s)}{\partial s^i \partial s^j} \Big|_{s_t} \right]. \end{aligned}$$

As we have rearranged the HJB equation so that the argument of expectation does not depend on the model, μ and σ , we can construct a temporal-difference update directly from it. We refer to this update as *differential temporal difference (dTD)* and expect it to be particularly effective when the observation interval Δt is small.

Definition 1 (differential temporal difference). Let $\Delta t > 0$ be a time step and \widehat{V} denote an estimated value function. The dTD is defined as:

$$\begin{aligned} \text{dTD} := & \frac{1}{\gamma} \left(\rho(s_t, a_t) + \sum_{i=1}^n \frac{s_{t+\Delta t}^i - s_t^i}{\Delta t} \frac{\partial \widehat{V}(s)}{\partial s^i} \Big|_{s_t} \right. \\ & \left. + \frac{1}{2} \sum_{i=1}^n \sum_{j=1}^n \frac{(s_{t+\Delta t}^i - s_t^i)(s_{t+\Delta t}^j - s_t^j)}{\Delta t} \frac{\partial^2 \widehat{V}(s)}{\partial s^i \partial s^j} \Big|_{s_t} \right) - \widehat{V}(s_t). \end{aligned} \quad (9)$$

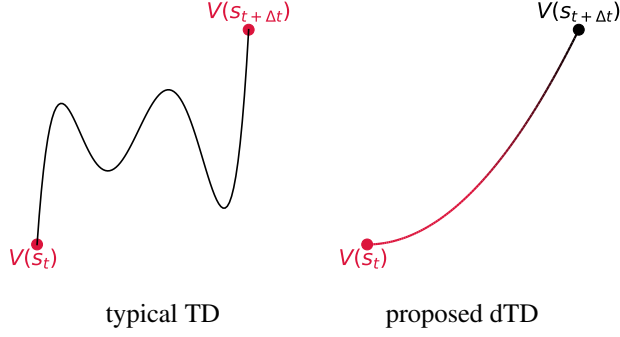


Figure 1: Qualitative difference between the typical TD method and the proposed dTD method; the objects in red indicate what is adjusted by each temporal difference. (Left) In the typical TD method, the values of \hat{V} are adjusted to minimize the TD error. (Right) In the dTD method, the gradient and the second derivative of \hat{V} at s_t are adjusted to minimize the dTD error.

As illustrated in Figure 1, unlike conventional TD methods based on transition kernels, dTD encourages the learning of a smooth value function by incorporating the continuity of the state space, even under sample-based approximation. We note that the version of dTD for ODE systems can be recovered by simply removing the term corresponding to the diffusion coefficient σ .

4.2 Contraction Property of the HJB Operator

To enable theoretical analysis of dTD learning, we investigate whether the HJB operator under a fixed policy satisfies a contraction property. Recent work has established PAC-learnability and convergence guarantees for classical TD learning under both linear and nonlinear function approximation Cai et al. (2019); Li et al. (2024); algorithmically, our method differs from these results only in that the TD update is replaced by its differential counterpart. For error analysis, we regard the contractivity of the Bellman operator as the key property of TD; other assumptions pertain to the underlying MDP or to restrictions on the hypothesis class, not to TD itself. Accordingly, we restrict our attention to showing that the HJB operator under a fixed policy is a contraction under certain assumptions. It alone will be sufficient for subsequent error bounding.

Definition 2 (HJB operator under a fixed policy). *Given a stationary Markov policy $\pi : S \rightarrow A$, discount rate $\gamma > 0$, drift $\mu : S \times A \rightarrow \mathbb{R}^n$, diffusion $\sigma : S \times A \rightarrow \mathbb{R}^{n \times m}$, and instantaneous reward rate $\rho : S \times A \rightarrow \mathbb{R}$, the HJB operator under a fixed policy T maps any function $V : S \rightarrow \mathbb{R}$ to*

$$(TV)(s_t) := \frac{1}{\gamma} \mathbb{E}_{p_\pi} \left[\rho(s_t, a_t) + \sum_{i=1}^n \mu^i(s_t, a_t) \frac{\partial V(s)}{\partial s^i} \Big|_{s_t} + \frac{1}{2} \sum_{i=1}^n \sum_{j=1}^m [\sigma(s_t, a_t) \sigma^\top(s_t, a_t)]^{ij} \frac{\partial^2 V(s)}{\partial s^i \partial s^j} \Big|_{s_t} \right].$$

We next show that T is a contraction under certain conditions. A proof is deferred to Appendix A.3.

Proposition 2 (Contraction property). *Assume the following conditions hold:*

- (i) *The value function V is L_V -Lipschitz continuous and β_V -smooth;*
- (ii) *The drift μ and diffusion σ are L_μ - and L_σ -Lipschitz continuous, respectively;*
- (iii) *The state and action spaces are bounded: $\|(s, a)\|_\infty < B$; and*
- (iv) *The discount factor γ satisfies $nL_V B_1(L_\mu) + \frac{1}{2}n^2\beta_V m B_2(L_\sigma) < \gamma$, where*

$$B_1(L_\mu) := \|\mu(0, 0)\|_\infty + L_\mu B \quad \text{and} \quad B_2(L_\sigma) := (\|\sigma(0, 0)\|_\infty + L_\sigma B)^2,$$

then the HJB operator under a fixed policy is a contraction.

We note about the interpretation and practicality of each of the four assumptions in Proposition 2 as follows: (i) Since the HJB equation is interpreted in the viscosity sense, and its solution may lack differentiability, imposing Lipschitz continuity and smoothness requires more careful justification. (ii) The Lipschitz continuity of the drift and diffusion coefficients is a standard condition for the existence and uniqueness of solutions to the SDE (see Appendix A.1), and thus imposes no additional constraint. (iii) The boundedness of the state space is a common and practical modeling assumption, often justified by safety constraints or physical limitations in real-world systems. (iv) The discount factor γ is a tunable parameter. Even in high-dimensional problems (i.e., large n or m), one can choose γ sufficiently large to satisfy this assumption. However, increasing γ shortens the effective planning horizon and may overly emphasize short-term rewards, so practical trade-offs must be considered.

5 Method

This section outlines our method for applying dTD in deep reinforcement learning. Because dTD relies on function approximation, we restrict our attention to the deep RL regime, representing the value function with a neural network. A concise pseudocode listing is provided in Appendix B.1; here we explain the loss formulation and the β -dTD stabilization strategy.

5.1 Loss function

In deep RL, TD methods typically use a fixed target, known as the TD target, $r(s, t) + \gamma_{\text{discrete}} V(s_{t+1})$, as the teacher and aim to approximate the prediction $V(s_t)$ by minimizing the squared error between them. Although it may seem natural, by analogy with classical TD, to treat the $V(s_t)$ term in the dTD (9) as the prediction and regard the remaining terms as the dTD target, this is in fact unnecessary. As shown in Appendix A.2, the terms that appear in (4) and thus in (9) are derived through a series of transformations, and thus in dTD we no longer interpret the terms other than $V(s_t)$ as a low-variance estimate of the Bellman error. Consequently, the split between prediction and target is not unique.

We examine two different ways of defining the prediction and target from the rhs of (9).

- As a baseline, we first consider a naive formulation following the typical TD-style decomposition, that is, we treat $V(s_t)$ as the prediction. We refer to this approach as **naive-dTD**.
- On the other hand, inspired by the Taylor expansion of the Bellman equation, we treat the terms involving the derivative of $V(s_t)$ as the prediction and regard the rest as the target. We term such a more motivated parametrization simply as **dTD** hereafter.

These two variants are summarized in Table 1. As introduced in the next section, we empirically found that dTD performed significantly better than naive-dTD.

5.2 Hybrid scheme for stabilizing dTD

Although Proposition 2 establishes a contraction result, the Lipschitz and smoothness constants are unknown in practice, so we cannot a priori guarantee that plain dTD operates inside the contraction regime. To make the critic update more robust, we linearly combine the classical TD error with the dTD error, using weights $1 - \beta$ and β , respectively; we call the resulting update β -dTD. The TD part supplies the empirical stability that underpins most deep RL algorithms, whereas the dTD part injects gradient information from the continuous dynamics, accelerating learning when the underlying assumptions are approximately satisfied. We hypothesize that it can strike a balance to stabilize learning progress and potentially improve convergence behavior in practice.

Table 1: Comparison of target and prediction terms in TD methods. Here, $\Delta s_t^i := s_{t+\Delta t}^i - s_t^i$ denotes the i -th component of the state transition over a small time interval Δt .

	Target	Prediction
TD	$r(s, t) + \gamma_{\text{discrete}} V(s_{t+1})$	$V(s_t)$
naive-dTD	$\frac{1}{\gamma} \left(\rho(s_t, a_t) + \sum_{i=1}^n \frac{\Delta s_t^i}{\Delta t} \frac{\partial V(s)}{\partial s^i} \Big _{s_t} + \frac{1}{2} \sum_{i=1}^n \sum_{j=1}^n \frac{\Delta s_t^i \Delta s_t^j}{\Delta t} \frac{\partial^2 V(s)}{\partial s^i \partial s^j} \Big _{s_t} \right)$	$V(s_t)$
dTD	$-\rho(s_t, a_t) + \gamma V(s_{t+\Delta t})$	$\sum_{i=1}^n \frac{\Delta s_t^i}{\Delta t} \frac{\partial V(s)}{\partial s^i} \Big _{s_t} + \frac{1}{2} \sum_{i=1}^n \sum_{j=1}^n \frac{\Delta s_t^i \Delta s_t^j}{\Delta t} \frac{\partial^2 V(s)}{\partial s^i \partial s^j} \Big _{s_t}$

5.3 Efficient Computation of the dTD Loss

Since equation (9) involves the Hessian, it may seem that $O(n^2)$ (where n is the dimension of the observation space) computations are required. However, by rearranging the order of calculations, such as using

$$\left\langle \Delta s_t, \frac{\partial^2 V(s)}{\partial s^2} \Big|_{s_t} \Delta s_t \right\rangle = \left\langle \Delta s_t, \frac{\partial}{\partial s} \left\langle \frac{\partial V}{\partial s}, \Delta s_t \right\rangle \Big|_{s_t} \right\rangle,$$

we can avoid directly calculating the Hessian and achieve a computation complexity of $O(n)$.

6 Experiments

6.1 Modification for discrete environment compatibility

In our theoretical framework, we work with continuous rewards (i.e., reward rate function) and a specific form of the discount ratio $e^{-\gamma}$, which is not directly compatible with the discrete discount ratio γ_{discrete} . To address this, we adjusted the reward and discount ratio following the same approach discussed in Tallec et al. (2019). The continuous reward formulation can be approximated by:

$$\int_0^\infty e^{-\gamma t} \rho(s_t, a_t) dt \approx \sum_{k=0}^\infty e^{(-\gamma \Delta t)k} \rho(s_{k\Delta t}, a_{k\Delta t}) \Delta t.$$

In this approximation, $\rho(s_t, a_t) \Delta t$ corresponds to the discrete reward r , and $e^{-\gamma \Delta t}$ corresponds to the discrete discount ratio γ_{discrete} . Thus, we can establish the following relationship:

$$\rho(s_t, a_t) = \frac{r(s_t, a_t)}{\Delta t} \quad \text{and} \quad \gamma = -\frac{1}{\Delta t} \log(\gamma_{\text{discrete}}).$$

This adjustment ensures that the observed discrete rewards are properly scaled to align with the continuous reward formulation used in the dTD method. With this scaling, dTD can be computed as

$$\begin{aligned} \text{dTD Target : } & -r(s_t, a_t) - \log(\gamma_{\text{discrete}})V(s_{t+\Delta t}) \quad \text{and} \\ \text{dTD Prediction : } & \sum_{i=1}^n (s_{t+\Delta t}^i - s_t^i) \frac{\partial V(s)}{\partial s_i} \Big|_{s_t} + \frac{1}{2} \sum_{i=1}^n \sum_{j=1}^n (s_{t+\Delta t}^i - s_t^i)(s_{t+\Delta t}^j - s_t^j) \frac{\partial^2 V(s)}{\partial s_i \partial s_j} \Big|_{s_t}. \end{aligned}$$

6.2 Experiment design

Environment We conducted experiments with the Brax¹ library (Freeman et al., 2021) in the following environments: Hopper, HalfCheetah, Ant and Humanoid. Each environment provides a mid- to high-dimensional state space, with the number of state components varying across environments: Hopper (11 dimensions), HalfCheetah (17 dimensions), Ant (27 dimensions) and Humanoid (244 dimensions). In each environment, at every step, we perturbed each state component by adding noise in the form of

$$s_i \leftarrow s_i + \text{coef} \times |s_i| \times \text{noise},$$

where $\text{noise} \sim \mathcal{N}(0, 1)$, and tested for three values of $\text{coef} = 0.00, 0.01, 0.05$. By adding this process noise, we aim to simulate with SDE systems, with the case of $\text{coef} = 0.00$ representing the limit case corresponding to ODEs. The specific time-step values used for each environment, which are not directly used in the learning process but are important to ensure they are small enough, are: Hopper: $\Delta t = 0.008$, HalfCheetah: $\Delta t = 0.05$, Ant: $\Delta t = 0.05$ and Humanoid: $\Delta t = 0.015$.

Baseline Various methods have been developed specifically for settings such as ODE (Tallec et al., 2019), LQR (Vamvoudakis and Crofton, 2017), or time-dependent Q functions with finite horizons (Jia and Zhou, 2023), but are often incompatible with the current deep RL framework (Kim et al., 2021) or rely on model-based assumptions (Munos and Bourguine, 1997), making them unsuitable for comparison with our proposed method. We chose to use standard TD methods as baselines and experimented with TD, β -naive-dTD, and β -dTD, using PPO (Schulman et al., 2017).

Hyperparameter tuning For hyperparameter tuning, we applied the DEHB (Awad et al., 2021), a multi-fidelity method that is currently considered the most effective method in RL (Eimer et al., 2023). While we performed hyperparameter tuning for the standard PPO algorithm as well, we also reference the official tuning results from Freeman et al. (2021) for fair comparison. Additional details about the hyperparameter search space can be found in Appendix B.

¹<https://github.com/google/brax>

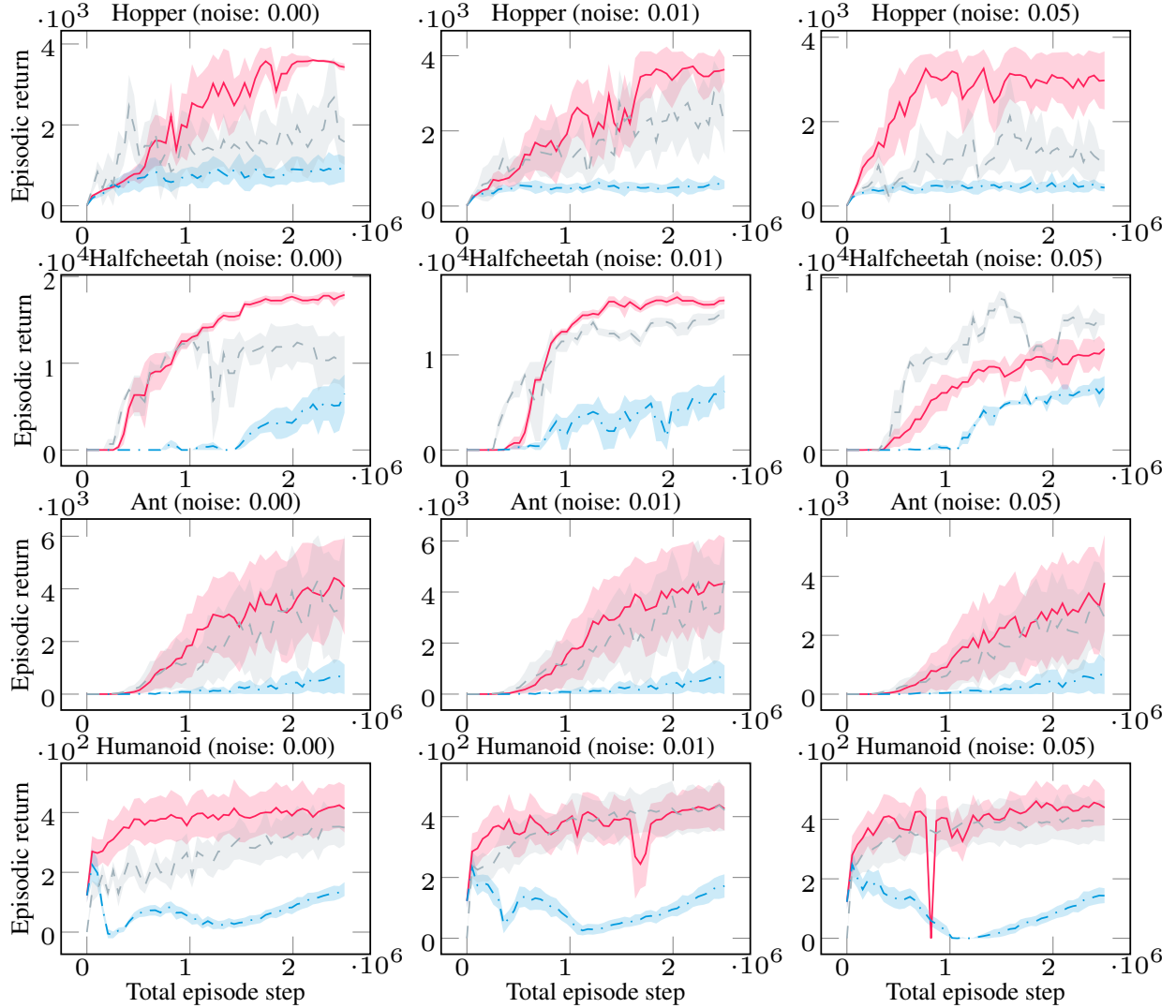


Figure 2: Performance of TD, β -naive-dTD, and β -dTD on continuous control benchmark. Each column corresponds to different noise levels (coef = 0.00, 0.01, 0.05), and each row corresponds to different environments. The tuned β values for β -naive-dTD were 0.08, 0.07, 0.23, 0.02 and for β -dTD were 0.57, 0.74, 0.24, 0.33 in Hopper, HalfCheetah, Ant, and Humanoid, respectively.

6.3 Results and discussion

Comparative evaluation We compare (the variants of) the proposed method and the baseline:

(β -naive-dTD vs. β -dTD) In Figure 2, we can observe that β -dTD consistently outperforms β -naive-dTD.

In all the environments, the optimized values of β for β -naive-dTD were quite small, suggesting that the effective update rule of β -naive-dTD became close to that of the standard TD. Despite such a fact, however, the performance of β -naive-dTD remains significantly worse than the standard TD. There are two possible explanations: (1) the β value chosen for β -naive-dTD was actually still not small enough to fully eliminate the adverse effect of the naive-dTD term; and (2) the TD-related parameters in β -naive-dTD were only suboptimally tuned because hyperparameter tuning resources were allocated mainly to optimizing β . These factors may jointly account for the unexpectedly poor performance of β -naive-dTD.

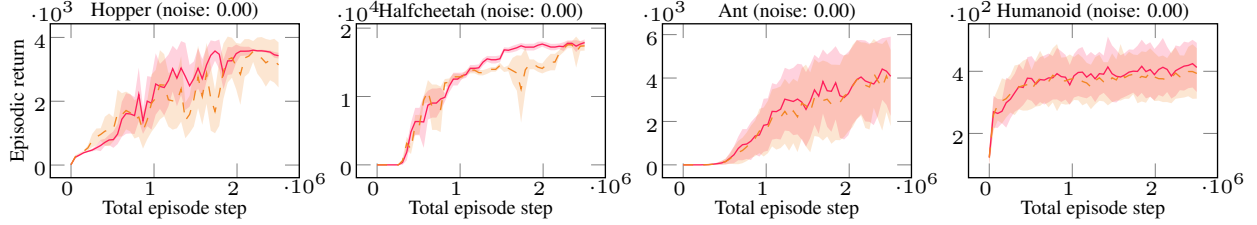


Figure 3: Performance comparison of β -dTD with the diffusion term and without the diffusion term, under deterministic dynamics (noise level 0.00).

(TD vs. β -dTD) As shown in Figure 2, β -dTD outperforms TD or achieves comparable performance in all cases. While the degree of improvement varies, the final performance of TD and β -dTD tends to converge, which is not very surprising because both dTD and TD are derived from the same Bellman equation, and the resulting value functions should thus be similar to each other eventually. Nevertheless, dTD has the advantage of implicitly utilizing continuity information during training, which enables it to make more informative updates. Consequently, although the final performance may be comparable, β -dTD tends to show a faster rate of improvement relative to TD.

Significance of dTD In contrast to β -naive-dTD, the weight β in β -dTD is not exceedingly small. Notably, in the Halfcheetah environment, β assumes a relatively large value of 0.74. This indicates that dTD retains a meaningful impact on the learning process.

Impact of process noise In terms of robustness to process noise, both β -dTD and TD exhibit similar performance. When the noise level is $\text{coef} = 0.01$, neither method experiences significant degradation in performance. However, when the noise level is increased to $\text{coef} = 0.05$, both β -dTD and TD show similar reduction in performance, particularly in environments like Ant and Halfcheetah.

Using the diffusion term for sample-induced perturbations Figure 3 shows a comparison between β -dTD variants with and without the diffusion term under deterministic dynamics (i.e., noise level 0.00). Somewhat unexpectedly, retaining the diffusion term achieves consistently better performance. It suggests that even in the absence of process noise, incorporating the diffusion term is beneficial. It is probably because the diffusion term helps account for perturbations due to finite-sample approximation. These results highlight that the SDE-based formulation of dTD can improve learning effectiveness even in nominally deterministic settings.

7 Conclusion

We have presented differential TD (dTD), a temporal difference method based on the HJB equation. In contrast to approaches based on transition kernels, the proposed method can incorporate the continuity of dynamics into the learning process without knowing the dynamics. We have shown empirical results for a variety of continuous control environments with different time intervals. The empirical results highlight the potential advantages of dTD in terms of learning speed and efficiency while also implying that stability concerns may exist. Although the current paper focuses on the theoretical development of dTD, these observations are useful and also warrant further empirical exploration.

We have also analyzed the conditions under which the HJB operator is a contraction mapping. This contraction property is crucial for proving the convergence of the proposed method. However, a drawback is

that the sufficient conditions we identify, such as the requirement of a large discount factor depending on the state space dimension, are not always easy to verify or satisfy in practice. Future work includes enforcing contraction through architectural design or Lipschitz regularization to guarantee convergence, reducing the variance of learning by improved estimators or regularization, and extending the wide range of existing TD-based techniques to the dTD framework.

References

- Leemon C. Baird. Reinforcement learning in continuous time: Advantage updating. In *Proceedings of 1994 IEEE International Conference on Neural Networks*, volume 4, pages 2448–2453, 1994.
- Rémi Munos. A convergent reinforcement learning algorithm in the continuous case based on a finite difference method. In *Proceedings of the 15th International Joint Conference on Artificial Intelligence*, volume 2, pages 826–831, 1997.
- Rémi Munos and Paul Bourgin. Reinforcement learning for continuous stochastic control problems. In *Advances in Neural Information Processing Systems*, volume 10, 1997.
- Kenji Doya. Reinforcement learning in continuous time and space. *Neural Computation*, 12(1):219–245, 2000.
- Rémi Munos. Policy gradient in continuous time. *Journal of Machine Learning Research*, 7(27):771–791, 2006.
- Emanuel Todorov, Tom Erez, and Yuval Tassa. Mujoco: A physics engine for model-based control. pages 5026–5033, 2012.
- Jens Kober, J Andrew Bagnell, and Jan Peters. Some studies in machine learning using the game of checkers. *The International Journal of Robotics Research*, 32(11):1238–1274, 2013.
- John Schulman, Sergey Levine, Philipp Moritz, Michael Jordan, and Pieter Abbeel. Trust region policy optimization. In *Proceedings of the 32nd International Conference on Machine Learning*, pages 1889–1897, 2015.
- Volodymyr Mnih, Adrià Puigdomènech Badia, Mehdi Mirza, Alex Graves, Tim Harley, Timothy P. Lillicrap, David Silver, and Koray Kavukcuoglu. Asynchronous methods for deep reinforcement learning. In *Proceedings of the 33rd International Conference on Machine Learning*, pages 1928–1937, 2016.
- Kyriakos G. Vamvoudakis and Kevin T. Crofton. Q-learning for continuous-time linear systems: A model-free infinite horizon optimal control approach. *Systems & Control Letters*, 100:14–20, 2017.
- John Schulman, Filip Wolski, Prafulla Dhariwal, Alec Radford, and Oleg Klimov. Proximal policy optimization algorithms. arXiv:1707.06347, 2017.
- Tuomas Haarnoja, Aurick Zhou, Pieter Abbeel, and Sergey Levine. Soft actor-critic: Off-policy maximum entropy deep reinforcement learning with a stochastic actor. In *Proceedings of the 35th International Conference on Machine Learning*, pages 1861–1870, 2018.
- David Silver, Thomas Hubert, Julian Schrittwieser, Ioannis Antonoglou, Matthew Lai, Arthur Guez, Marc Lanctot, Laurent Sifre, Dhharshan Kumaran, Thore Graepel, Timothy Lillicrap, Karen Simonyan, and Demis Hassabis. Mastering chess and shogi by self-play with a general reinforcement learning algorithm. arXiv:1712.01815, 2018.

- Danijar Hafner, Timothy Lillicrap, and Jimmy Ba. Dream to control: Learning behaviors by latent imagination. arXiv: 1912.01603, 2019.
- Corentin Tallec, Léonard Blier, and Yann Ollivier. Making deep Q-learning methods robust to time discretization. In *Proceedings of the 36th International Conference on Machine Learning*, pages 6096–6104, 2019.
- Qi Cai, Zhuoran Yang, Jason Lee, and Zhaoran Wang. Neural temporal-difference learning converges to global optima. In *Advances in Neural Information Processing Systems 32*, 2019.
- Haoran Wang, Thaleia Zariphopoulou, and Xun Yu Zhou. Reinforcement learning in continuous time and space: A stochastic control approach. *Journal of Machine Learning Research*, 21(198), 2020.
- Daniel Freeman, Erik Frey, Anton Raichuk, Sertan Girgin, Igor Mordatch, and Olivier Bachem. Brax - a differentiable physics engine for large scale rigid body simulation. In *Proceedings of the Neural Information Processing Systems Track on Datasets and Benchmarks*, volume 1, 2021.
- Noor Awad, Neeratyoy Mallik, and Frank Hutter. DEHB: Evolutionary hyperband for scalable, robust and efficient hyperparameter optimization. In *Proceedings of the 30th International Joint Conference on Artificial Intelligence*, pages 2147–2153, 2021.
- Çağatay Yıldız, Markus Heinonen, and Harri Lähdesmäki. Continuous-time model-based reinforcement learning. In *Proceedings of the 38th International Conference on Machine Learning*, pages 12009–12018, 2021.
- Jeongho Kim, Jaekuk Shin, and Insoon Yang. Hamilton-Jacobi deep Q-learning for deterministic continuous-time systems with Lipschitz continuous controls. *Journal of Machine Learning Research*, 22(206), 2021.
- Wenpin Tang, Paul Yuming Zhang, and Xun Yu Zhou. Exploratory hjb equations and their convergence. *SIAM Journal on Control and Optimization*, 60, 2022.
- Yanwei Jia and Xun Yu Zhou. Policy evaluation and temporal–difference learning in continuous time and space: A martingale approach. *Journal of Machine Learning Research*, 23(154), 2022a.
- Yanwei Jia and Xun Yu Zhou. Policy gradient and actor-critic learning in continuous time and space: Theory and algorithms. *Journal of Machine Learning Research*, 23(275), 2022b.
- Yanwei Jia and Xun Yu Zhou. q-learning in continuous time. *Journal of Machine Learning Research*, 24(161), 2023.
- Hanyang Zhao, Wenpin Tang, and David D. Yao. Policy optimization for continuous reinforcement learning. volume 36, pages 13637–13663, 2023.
- Ziad Kobeissi and Francis Bach. Temporal difference learning with continuous time and state in the stochastic setting. arXiv:1712.01815, 2023.
- Theresa Eimer, Marius Lindauer, and Roberta Raileanu. Hyperparameters in reinforcement learning and how to tune them. In *Proceedings of the 40th International Conference on Machine Learning*, pages 9104–9149, 2023.
- Gen Li, Weichen Wu, Yuejie Chi, Cong Ma, Alessandro Rinaldo, and Yuting Wei. High-probability sample complexities for policy evaluation with linear function approximation. *IEEE Transactions on Information Theory*, 2024.

A Mathematical Details

A.1 Justification for the Continuous RL Formulation

In Section 3, we modeled the evolution of the state under a stochastic policy π by the controlled SDE

$$dS_t = \mu(S_t, A_t) dt + \sigma(S_t, A_t) dB_t, \quad A_t \sim \pi(\cdot | S_t).$$

Here, the control is applied in the form of action samples drawn from a stochastic policy at each time step. While this formulation closely reflects the sampling-based behavior in RL, it raises a technical challenge: the presence of external randomness in addition to the intrinsic Brownian noise introduces analytical difficulties. As a result, the well-definedness of this SDE is not immediately obvious.

To address this issue, many prior works (e.g., Wang et al. (2020); Jia and Zhou (2022a,b, 2023); Zhao et al. (2023)) adopt the averaged dynamics, denoted by $(\tilde{S}_t)_{t \geq 0}$, whose distribution at each time t is known to coincide with that of the original one under the same initial condition (Wang et al., 2020). Specifically, the averaged dynamics is defined as

$$d\tilde{S}_t = \tilde{\mu}(\tilde{S}_t, \pi) dt + \tilde{\sigma}(\tilde{S}_t, \pi) d\tilde{B}_t,$$

where $\tilde{\mu}(s, \pi) = \int_{\mathcal{A}} \mu(s, a) \pi(a) da$, $\tilde{\sigma}(s, a) = (\int_{\mathcal{A}} \sigma(s, a) \sigma^\top(s, a) \pi(a) da)^{\frac{1}{2}}$ and $(\tilde{B}_t)_{t \geq 0}$ is the m -dimensional Brownian motion. Since the averaged dynamics no longer involves the external randomness induced by stochastic action selection, its well-definedness is ensured by classical SDE theory under standard assumptions such as Lipschitz continuity and a linear growth condition.

Since the marginal distributions of the two dynamics coincide, the corresponding value functions also coincide:

$$\begin{aligned} V^\pi(s) &= \mathbb{E}_{p_\pi} \left[\int_t^\infty e^{-\gamma(\tau-t)} \rho(S_\tau, A_\tau) d\tau \mid S_t = s \right] \\ &= \mathbb{E}_{\tilde{p}} \left[\int_t^\infty e^{-\gamma(\tau-t)} \tilde{\rho}(\tilde{S}_\tau, \pi) d\tau \mid \tilde{S}_t = s \right] \\ &=: \tilde{V}^\pi(s), \end{aligned}$$

where $\tilde{\rho}(s, \pi) := \int_{\mathcal{A}} \rho(s, a) \pi(a) da$. Moreover, it has been shown in Zhao et al. (2023) that the value function \tilde{V}^π , and hence V^π , is the unique viscosity solution to the HJB equation (4), under the assumptions listed below. This confirms that the value function V^π used in the main text—defined via the original, sampling-based dynamics—is theoretically justified.

We summarize the required assumptions below for completeness:

Assumption 1 (Adapted from (Zhao et al., 2023)). *Assume the following:*

- (i) μ , σ and ρ are all continuous functions in their respective arguments.
- (ii) μ and ρ are uniformly Lipschitz continuous in their first argument: for some constant $C > 0$,

$$\|\phi(s, a) - \phi(s', a)\| \leq C \|s - s'\| \quad \text{for all } a \in \mathcal{A}, \phi \in \{\mu, \rho\},$$

- (iii) The averaged diffusion matrix $\tilde{\sigma}(s, \pi)^2$ is uniformly elliptic: there exist $0 < \sigma_0 < \bar{\sigma}_0$ such that

$$\sigma_0^2 I \preceq \tilde{\sigma}^2(s, \pi) \preceq \bar{\sigma}_0^2 I \quad \text{for all } s \in \mathcal{S}.$$

- (iv) The averaged SDE admits a weak solution that is unique in law.

(v) The policy $\pi(a \mid s)$ is measurable and uniformly Lipschitz continuous in s :

$$\int_A |\pi(a \mid s) - \pi(a \mid s')| da \leq C \|s - s'\|.$$

Accordingly, in the stochastic setting, we assume that the diffusion term is non-degenerate. This does not mean that the noise-free setting is ill-posed; rather, well-posedness in that case can be established via the theory of first-order HJB equations.

A.2 Ito formula

The Bellman equation is given by:

$$V^*(s_t) = \max_{\pi} \mathbb{E}_{p_{\pi}} [\rho(s_t, A_t) \Delta t + e^{-\gamma \Delta t} V^*(S_{t+\Delta t})].$$

Assuming that a stochastic process $(S_t)_{t \geq 0}$ follows the SDE (1), the term $V^*(S_{t+\Delta t})$ can be further expanded using Itô's lemma:

$$\begin{aligned} V^*(s_t) &= \max_{\pi} \mathbb{E}_{p_{\pi}} \left[\rho(s_t, A_t) \Delta t + e^{-\gamma \Delta t} V^*(S_{t+\Delta t}) \right] \\ &= \max_{\pi} \mathbb{E}_{p_{\pi}} \left[\rho(s_t, A_t) \Delta t + e^{-\gamma \Delta t} \left(V^*(s_t) + \sum_{i=1}^n \mu^i(s_t, A_t) \frac{\partial V^*(s)}{\partial s_i} \Big|_{s_t} \right. \right. \\ &\quad \left. \left. + \frac{1}{2} \sum_{i=1}^n \sum_{j=1}^n [\sigma(s_t, A_t) \sigma^{\top}(s_t, A_t)]^{ij} \frac{\partial^2 V^*(s)}{\partial s_i \partial s_j} \Big|_{s_t} \right. \right. \\ &\quad \left. \left. + \sum_{i=1}^n \sum_{j=1}^m \sigma_j^i(s_t, A_t) \frac{\partial V^*(s)}{\partial s_i} \Big|_{s_t} (B_{t+\Delta t}^j - B_t^j) + O((\Delta t)^{3/2}) \right) \right] \\ &= \max_{\pi} \mathbb{E}_{p_{\pi}} \left[\rho(s_t, A_t) \Delta t + e^{-\gamma \Delta t} \left\{ V^*(s_t) + \left(\sum_{i=1}^n \mu^i(s_t, A_t) \frac{\partial V^*(s)}{\partial s_i} \Big|_{s_t} \right. \right. \right. \\ &\quad \left. \left. \left. + \frac{1}{2} \sum_{i=1}^n \sum_{j=1}^n [\sigma(s_t, A_t) \sigma^{\top}(s_t, A_t)]^{ij} \frac{\partial^2 V^*(s)}{\partial s_i \partial s_j} \Big|_{s_t} \right) \Delta t + O((\Delta t)^{3/2}) \right\} \right]. \end{aligned}$$

Simplifying the equation and taking the limit as $\Delta t \rightarrow 0$, we have the condition for the optimal value function:

$$\begin{aligned} V^*(s_t) &= \frac{1}{\gamma} \max_{\pi} \mathbb{E}_{p_{\pi}} \left[\rho(s_t, A_t) + \sum_{i=1}^n \mu^i(s_t, A_t) \frac{\partial V^*(s)}{\partial s_i} \Big|_{s_t} \right. \\ &\quad \left. + \frac{1}{2} \sum_{i=1}^n \sum_{j=1}^n [\sigma(s_t, A_t) \sigma^{\top}(s_t, A_t)]^{ij} \frac{\partial^2 V^*(s)}{\partial s_i \partial s_j} \Big|_{s_t} \right]. \end{aligned}$$

A.3 Proof of Proposition 2

Proof.

$$\begin{aligned}
& \|TV_1^\pi(s) - TV_2^\pi(s)\|_\infty \\
& \leq \frac{1}{\gamma} \left\| \mathbb{E}_{p^\pi} \left[\sum_{i=1}^n \mu_i \left(\frac{\partial V_1^\pi}{\partial s_i} - \frac{\partial V_2^\pi}{\partial s_i} \right) + \frac{1}{2} \sum_{i=1}^n \sum_{j=1}^n [\sigma \sigma^\top]^{ij} \left(\frac{\partial^2 V_1^\pi}{\partial s_i \partial s_j} - \frac{\partial^2 V_2^\pi}{\partial s_i \partial s_j} \right) \right] \right\|_\infty \\
& \leq \frac{1}{\gamma} \left\| \sum_{i=1}^n \mu_i \left(\frac{\partial V_1^\pi}{\partial s_i} - \frac{\partial V_2^\pi}{\partial s_i} \right) + \frac{1}{2} \sum_{i=1}^n \sum_{j=1}^n [\sigma \sigma^\top]^{ij} \left(\frac{\partial^2 V_1^\pi}{\partial s_i \partial s_j} - \frac{\partial^2 V_2^\pi}{\partial s_i \partial s_j} \right) \right\|_\infty \\
& \leq \frac{1}{\gamma} \left(\sum_{i=1}^n |\mu_i| \left\| \left(\frac{\partial V_1^\pi}{\partial s_i} - \frac{\partial V_2^\pi}{\partial s_i} \right) \right\|_\infty + \frac{1}{2} \sum_{i=1}^n \sum_{j=1}^n |[\sigma \sigma^\top]^{ij}| \left\| \left(\frac{\partial^2 V_1^\pi}{\partial s_i \partial s_j} - \frac{\partial^2 V_2^\pi}{\partial s_i \partial s_j} \right) \right\|_\infty \right) \\
& \leq \frac{1}{\gamma} \left(\sum_{i=1}^n |\mu_i| L_V + \frac{1}{2} \sum_{i=1}^n \sum_{j=1}^n |[\sigma \sigma^\top]^{ij}| \beta_V \right) \|V_1^\pi(s) - V_2^\pi(s)\|_\infty. \tag{10}
\end{aligned}$$

The last step uses assumption (i). By assumptions (ii) and (iii),

$$\begin{aligned}
|\mu_i| & \leq \|\mu(s, A)\|_\infty \\
& \leq \|\mu(0, 0)\|_\infty + L_\mu \|s, A\|_\infty = B_1(L_\mu) \quad \text{and} \tag{11}
\end{aligned}$$

$$\begin{aligned}
|[\sigma \sigma^\top]^{ij}| & \leq m \max_i^j |\sigma_i^j|^2 = m \|\sigma(s, A)\|_\infty^2 \\
& \leq m (\|\sigma(0, 0)\|_\infty + L_\sigma \|s, A\|_\infty)^2 = m B_2(L_\sigma). \tag{12}
\end{aligned}$$

Combining (10)–(12) yields

$$\|TV_1^\pi(s) - TV_2^\pi(s)\|_\infty \leq \frac{1}{\gamma} \left(n L_V B_1(L_\mu) + \frac{1}{2} n^2 \beta_V m B_2(L_\sigma) \right) \|V_1^\pi(s) - V_2^\pi(s)\|_\infty.$$

This factor is strictly less than 1 by assumption (iv), so T is a contraction. \square

B Implementation Details

B.1 Algorithm

The procedures for policy evaluation are summarized in Algorithm 1.

Algorithm 1 Policy evaluation with dTD

Input: policy π **Output:** V_θ Initialize value function V_θ with random parameter θ **for** each training step **do**Initialize buffer $\mathcal{D} = \emptyset$ and initial state s_0 **for** each environment step **do** $a_t \sim \pi(\cdot | s_t)$ $s_{t+\Delta t} \sim p(\cdot | s_t, a_t)$ $\mathcal{D} \leftarrow \mathcal{D} \cup (s_t, a_t, s_{t+\Delta t}, \rho_t)$ **end for****for** each update step **do**Sample a batch of D random transitions from \mathcal{D} $\bar{\theta} \leftarrow \theta$ $y_d \leftarrow -\rho_t^d - \gamma V_{\bar{\theta}}(s_{t+\Delta t}^d)$

$$\text{pred}_d \leftarrow \sum_{i=1}^n \frac{(s_{t+\Delta t}^{d,i} - s_t^{d,i})}{\Delta t} \frac{\partial V_\theta(s)}{\partial s_i} \Big|_{s_t^d} + \frac{1}{2} \sum_{i=1}^n \sum_{j=1}^n \frac{(s_{t+\Delta t}^{d,i} - s_t^{d,i})(s_{t+\Delta t}^{d,j} - s_t^{d,j})}{\Delta t} \frac{\partial^2 V_\theta(s)}{\partial s_i \partial s_j} \Big|_{s_t^d}$$

Update parameter θ using gradient descent method $\theta \leftarrow \text{argmin}_\theta \frac{1}{D} \sum_{d=1}^D (y_d - \text{pred}_d)^2$ **end for****end for**

B.2 Hyperparameters

The search space of the hyperparameters is summarized in Table 2. The values chosen finally are summarized in Tables 3.

Table 2: Hyperparameter search space

Hyperparameter	Search Space
environment steps per update (number of parallel environment: 64)	{8, 16, 32}
number of epochs per update	range(5, 20)
minibatch size	{256, 512}
learning rate	log(interval(1e-6, 5e-3))
normalize advantage	{True, False}
gae lambda	interval(0.8, 0.9999)
clip range	interval(0.0, 0.9)
entropy coefficient	interval(0.0, 0.3)
value loss weight	interval(0.0, 1.0)
mixture ratio β	interval(0.0, 1.0)

B.3 Computing Infrastructure and Reproducibility

Computing infrastructure Experiments were conducted on a machine with four NVIDIA Tesla V100 GPUs (32GB each) and an Intel Xeon E5-2698 v4 CPU. Although all experiments can be executed on a

Table 3: Best hyperparameters for PPO with TD and β -dTD across environments

Hyperparameter	TD				β -dTD			
	Ant	Hopper	Halfcheetah	Humanoid	Ant	Hopper	Halfcheetah	Humanoid
environment steps/update	8	32	16	16	32	32	8	16
epochs/update	11	7	5	15	16	19	9	10
minibatch size	512	512	256	512	256	256	256	256
learning rate	3.71e-4	1.18e-3	5.93e-4	1.40e-3	7.94e-5	3.52e-4	3.29e-4	1.08e-3
normalize advantage	False	False	False	False	False	False	False	False
GAE lambda	0.935	0.886	0.833	0.999	0.805	0.998	0.908	0.888
clip range	0.425	0.439	0.268	0.063	0.520	0.075	0.040	0.713
entropy coefficient	0.162	0.121	0.018	0.021	0.133	0.046	0.011	0.002
value loss weight	0.711	0.049	0.513	0.091	0.274	0.675	0.268	0.054
mixture ratio β	—	—	—	—	0.241	0.572	0.742	0.332

single GPU, multiple GPUs were used to run independent trials in parallel for efficiency.

Training time Hyperparameter tuning typically took 6–9 hours depending on the environment. Training time for the final runs depended on the environment and ranged from 10 to 60 minutes.

Reproducibility All experiments were conducted with the random seed fixed in the training scripts. However, MuJoCo (accessed via Brax) uses its own internal random seed that is not directly controllable, so full determinism cannot be ensured. The code is available at https://github.com/4thhia/differential_TD for reproducibility.